J-SEPINSKY, B-WILLEMS, VICKY, AND RASIO@NORTHWESTERN.EDU
Preprint typeset using LaTeX style emulateapj v. 10/09/06



# INTERACTING BINARIES WITH ECCENTRIC ORBITS II. SECULAR ORBITAL EVOLUTION DUE TO NON-CONSERVATIVE MASS TRANSFER

J. F. Sepinsky, B. Willems, V. Kalogera, F. A. Rasio
Department of Physics and Astronomy, Northwestern University, 2145 Sheridan Road, Evanston, IL 60208
*j-sepinsky, b-willems, vicky, and rasio@northwestern.edu*

## ABSTRACT

We investigate the secular evolution of the orbital semi-major axis and eccentricity due to mass transfer in eccentric binaries, allowing for both mass and angular momentum loss from the system. Adopting a delta function mass transfer rate at the periastron of the binary orbit, we find that, depending on the initial binary properties at the onset of mass transfer, the orbital semi-major axis and eccentricity can either increase or decrease at a rate linearly proportional to the magnitude of the mass transfer rate at periastron. The range of initial binary mass ratios and eccentricities that leads to increasing orbital semi-major axes and eccentricities broadens with increasing degrees of mass loss from the system and narrows with increasing orbital angular momentum loss from the binary. Comparison with tidal evolution timescales shows that the usual assumption of rapid circularization at the onset of mass transfer in eccentric binaries is not justified, irrespective of the degree of systemic mass and angular momentum loss. This work extends our previous results for conservative mass transfer in eccentric binaries and can be incorporated into binary evolution and population synthesis codes to model non-conservative mass transfer in eccentric binaries.
*Subject headings:* Celestial mechanics, Stars: Binaries: Close, Stars: Mass Loss

## 1. INTRODUCTION

Many astrophysically interesting binary systems pass through at least one mass-transfer phase during the course of their evolution. These mass transfer episodes not only affect the internal evolution of the stellar components, but also impact the binary properties. In particular, changes in the mass ratio and transfer of linear and angular momentum between the stars cause changes in the orbital elements which affect the evolution of the binary and can cause a feedback on the mass transfer process.

In binaries with eccentric orbits, the stars are closest to each other at the periastron of their relative orbit, so that any mass transfer is expected to take place first during periastron passage. The standard assumption in current binary evolution and population synthesis codes to deal with such mass transfer phases is that the orbit circularizes instantaneously at the onset of mass transfer. This assumption is in contrast with recent theoretical findings (Sepinsky et al. 2007b) as well as observations of semi-detached binaries with non-zero orbital eccentricities (Petrova & Orlov 1999; Raguzova & Popov 2005).

Sepinsky et al. (2007b, hereafter Paper I) studied the orbital evolution due to mass transfer in eccentric binaries by deriving a set of perturbed equations of motion for the binary components, as outlined initially by Hadjidemetriou (1969). The authors found that, under the assumption of conservation of total system mass and orbital angular momentum, the orbital semi-major axis and eccentricity can increase as well as decrease, depending on the initial orbital elements, binary component masses, and donor rotation rate. Furthermore, the orbital evolution timescales can be short enough to compete with or enhance any tidally driven orbital evolution.

In this paper, we extend the analysis presented in Paper I to account for mass and angular momentum loss from the binary. In § 2 and 3, we briefly recall the relevant ingredients for the study of mass transfer in eccentric binaries derived in Paper I, and update the formalism to account for systemic mass and angular momentum loss. In §4, we present timescales for the evolution of the orbital semi-major axis and eccentricity due to mass transfer for different degrees of mass and angular momentum loss and we compare the timescales to the timescales of orbital evolution due to tidal dissipation. The final section is devoted to concluding remarks.

## 2. BASIC ASSUMPTIONS

We consider a close binary consisting of two stars with masses $M_1$ and $M_2$ in an eccentric orbit with period $P_{\rm orb}$, semi-major axis $a$, and eccentricity $e$. The stars are assumed to rotate uniformly with angular velocities $\vec{\Omega}_1$ and $\vec{\Omega}_2$ around an axis perpendicular to the orbital plane and in the same sense as the orbital motion. Since, in eccentric binaries, the magnitude of the orbital angular velocity $\vec{\Omega}_{\rm orb}$ is a periodic function of time, the stellar rotation rates cannot be synchronized with the orbital motion at all orbital phases.

At some time $t$, one of the stars is assumed to fill its Roche lobe initiating mass transfer to its companion through the inner Lagrangian point $L_1$. We assume this point to lie on the line connecting the mass centers of the stars, even though non-synchronous rotation may cause it to oscillate in the direction perpendicular to the orbital plane (Matese & Whitmire 1983). Since the donor's equatorial plane coincides with the plane of the orbit, the transferred mass can furthermore be assumed to remain in the orbital plane at all times. In what follows, we refer to the Roche lobe filling star as star 1 and to the companion star as star 2.

In Paper I, we assumed that all mass transfered by the donor was accreted by the companion, and that any orbital angular momentum transported by the transferred matter was immediately returned to the orbit (presum-

ably through an accretion disk). Here, we relax those assumptions and assume some fraction $\beta$ of the transferred mass to be lost from the system:

$$\dot{M}_T = \beta \dot{M}_1, \tag{1}$$

where $M_T = M_1 + M_2$ is the total system mass. Consequently, the amount of matter accreted by the companion is

$$\dot{M}_2 = -\gamma \dot{M}_1 \tag{2}$$

where $\gamma = 1 - \beta$. The angular momentum carried away by the mass lost from the system is parameterized in terms of the specific angular momentum of the orbit as

$$\dot{J}_{\rm orb} = \mu \frac{J_{\rm orb}}{M_T} \dot{M}_T. \tag{3}$$

In the particular case where the matter lost from the system carries the specific orbital angular momentum of the accretor, $\mu = M_1/M_2$ (e.g., Kolb et al. 2001). For our purpose, we assume that no other sources of angular momentum loss besides mass loss are operating on the system. Any other sinks of orbital angular momentum such as tidal interactions, magnetic braking, and gravitational radiation can, at the lowest order of approximation, be added to Eq. (3) and Eqs. (18)–(19) derived in the next section to obtain the total rate of change of the orbital angular momentum and of the orbital elements.

With these assumptions, the equations governing the motion of the two stars around their common center of mass can be written in the form of a perturbed two-body problem as

$$\frac{d^2\vec{r}}{dt^2} = -\frac{G\left(M_1+M_2\right)}{|\vec{r}|^3}\vec{r} + S\,\hat{x} + T\,\hat{y} + W\,\hat{z}, \tag{4}$$

where $G$ is the Newtonian constant of gravitation, $\vec{r}$ is the position vector of the accretor with respect to the donor, $\hat{x}$ is a unit vector in the direction of $\vec{r}$, $\hat{y}$ is a unit vector in the orbital plane perpendicular to $\vec{r}$ in the direction of the orbital motion, and $\hat{z}$ is a unit vector perpendicular to the orbital plane parallel to and in the same direction as $\vec{\Omega}_{\rm orb}$. The functions $S$, $T$, and $W$ are the components of the perturbing force arising from the mass transfer between the binary components. They can be shown to be equal to

$$\begin{aligned} S =& \frac{f_{2,x}}{M_2} - \frac{f_{1,x}}{M_1} + \frac{\dot{M}_2}{M_2}\left(v_{\delta M_2,x} - |\vec{\Omega}_{\rm orb}||\vec{r}_{A_2}|\sin\phi\right) \\ & - \frac{\dot{M}_1}{M_1}v_{\delta M_1,x} + \frac{\ddot{M}_2}{M_2}|\vec{r}_{A_2}|\cos\phi - \frac{\ddot{M}_1}{M_1}|\vec{r}_{A_1}|, \end{aligned} \tag{5}$$

$$\begin{aligned} T =& \frac{f_{2,y}}{M_2} - \frac{f_{1,y}}{M_1} + \frac{\dot{M}_2}{M_2}\left(v_{\delta M_2,y} + |\vec{\Omega}_{\rm orb}||\vec{r}_{A_2}|\cos\phi\right) \\ & - \frac{\dot{M}_1}{M_1}\left(v_{\delta M_1,y} + |\vec{\Omega}_{\rm orb}||\vec{r}_{A_1}|\right) + \frac{\ddot{M}_2}{M_2}|\vec{r}_{A_2}|\sin\phi, \end{aligned} \tag{6}$$

$$W = \frac{f_{2,z}}{M_2} - \frac{f_{1,z}}{M_1}, \tag{7}$$

where $A_1$ denotes the point on the donor's surface from which mass is lost (the $L_1$ point), $A_2$ denotes the point on the accretor's surface at which mass is accreted, $\vec{r}_{A_1}$ and $\vec{r}_{A_2}$ are the position vectors of $A_1$ and $A_2$ with respect to the donor's and the accretor's center of mass, respectively, and the subscripts $x$, $y$, and $z$ denote vector components in the $\hat{x}$, $\hat{y}$, and $\hat{z}$ directions. Moreover, $\vec{f}_1$ is the gravitational force exerted by particles in the mass transfer stream on the donor star, $\vec{f}_2$ the gravitational force exerted by particles in the mass transfer stream on the accretor, $\vec{v}_{\delta M_1}$ the velocity of the matter ejected at $L_1$ with respect to the mass center of the donor star, $\vec{v}_{\delta M_2}$ the velocity of the accreted matter at $A_2$ with respect to the mass center of the accretor, and $\phi$ the angle between $\hat{x}$ and the vector from the center of mass of the accretor to $A_2$. More details can be found in Paper I.

## 3. ORBITAL EVOLUTION EQUATIONS

### 3.1. *Secular Variation of the Orbital Elements*

The perturbing force with components $S$, $T$, and $W$ in the equations governing the motion of the two stars around their common center of mass causes changes in the orbital semi-major axis $a$ and eccentricity $e$ at rates given by (e.g., Sterne 1960; Brouwer & Clemence 1961; Danby 1962; Fitzpatrick 1970)

$$\frac{da}{dt} = \frac{2}{n(1-e^2)^{1/2}}[Se\sin\nu + T(1+e\cos\nu)], \tag{8}$$

$$\begin{aligned} \frac{de}{dt} =& \frac{(1-e^2)^{1/2}}{na} \\ & \times\left\{S\sin\nu + T\left[\frac{2\cos\nu + e\left(1+\cos^2\nu\right)}{1+e\cos\nu}\right]\right\}, \end{aligned} \tag{9}$$

where $n = 2\pi/P_{\rm orb}$ is the mean motion, and $\nu$ the true anomaly. The long-term secular evolution of the orbital elements is obtained by averaging these equations over one orbital period:

$$\left\langle\frac{da}{dt}\right\rangle_{\rm sec} \equiv \frac{1}{P_{\rm orb}}\int_{-P_{\rm orb}/2}^{P_{\rm orb}/2}\frac{da}{dt}\,dt, \tag{10}$$

$$\left\langle\frac{de}{dt}\right\rangle_{\rm sec} \equiv \frac{1}{P_{\rm orb}}\int_{-P_{\rm orb}/2}^{P_{\rm orb}/2}\frac{de}{dt}\,dt. \tag{11}$$

As in Paper I, the integrals are most conveniently computed in terms of the true anomaly $\nu$.

### 3.2. *Orbital Angular Momentum Loss*

The perturbing functions $S$ and $T$ depend on the properties of the mass transfer stream. Calculation of the orbital semi-major axis and eccentricity evolution therefore, in principle, requires the calculation of the trajectories of the particles in the stream. In Paper I we bypassed such a calculation by assuming conservation of total system mass and orbital angular momentum. Here, we relax this assumption and generalize the formalism presented in Paper I by parameterizing systemic mass and angular momentum loss by means of Eqs. (2) and (3).

As shown in Paper I, the rate of change of the orbital angular momentum is related to the perturbing function $T$ by

$$\frac{\dot{J}_{\rm orb}}{J_{\rm orb}} = \frac{\dot{M}_1}{M_1} + \frac{\dot{M}_2}{M_2} - \frac{1}{2}\frac{\dot{M}_T}{M_T} + \frac{\left(1-e^2\right)^{1/2}}{na(1+e\,\cos\nu)}T. \tag{12}$$

If the only sink of orbital angular momentum is mass loss from the system, elimination of $\dot{J}_{\rm orb}$ from this equation and Eq. (3) yields

$$\left(\mu+\frac{1}{2}\right)\frac{\dot{M}_T}{M_T} - \frac{\dot{M}_1}{M_1} - \frac{\dot{M}_2}{M_2} = \frac{\left(1-e^2\right)^{1/2}}{na(1+e\,\cos\nu)}T. \tag{13}$$

## 4. ORBITAL EVOLUTION TIMESCALES

Since in binaries with eccentric orbits, mass transfer is expected to occur first at the periastron of the binary orbit, we approximate the mass transfer rate by a Dirac delta function as

$$\dot{M}_1 = \dot{M}_0\,\delta\left(\nu\right), \tag{14}$$

where $\dot{M}_0 < 0$ is the instantaneous mass transfer rate, and $\delta(\nu)$ the Dirac delta function.

To calculate the rates of secular change of the orbital semi-major axis and eccentricity, we neglect the gravitational force exerted by the particles in the mass-transfer stream on the binary components and set

$$f_{1,x} = f_{2,x} = 0, \tag{15}$$

$$f_{1,y} = f_{2,y} = 0. \tag{16}$$

With these assumptions, elimination of the perturbing function $T$ between Eqs. (6) and (13), and averaging over one orbital period yields

$$\begin{aligned}
&\gamma q v_{\delta M_2,y} + v_{\delta M_1,y} = -|\vec{\Omega}_{\rm orb,P}||\vec{r}_{A_1,P}| \\
&- na\left(\frac{1+e}{1-e}\right)^{1/2}\left[\gamma q - 1 + (1-\gamma)\left(\mu+\frac{1}{2}\right)\left(\frac{q}{1+q}\right)\right] \\
&- \gamma q|\vec{\Omega}_{\rm orb,P}||\vec{r}_{A_2}|\cos\phi_P\left[1-\left(\frac{d\phi}{d\nu}\right)_P\right],
\end{aligned} \tag{17}$$

where the subscript $P$ indicates quantities evaluated at periastron, and $q = M_1/M_2$ is the binary mass ratio. In the limiting case of conservative mass transfer ($\gamma = 1$), Eq. (17) reduces to Eq. (35) in Paper I.

Finally, we substitute Eqs. (15)–(17) into Eqs. (10) and (11) to derive the following rates of secular change of the orbital semi-major axis and eccentricity due to mass transfer at the periastron of eccentric binaries:

$$\begin{aligned}
\left\langle\frac{da}{dt}\right\rangle_{\rm sec} = \;& \frac{a}{\pi}\frac{\dot{M}_0}{M_1}\frac{1}{(1-e^2)^{1/2}} \\
&\times\left[e\frac{|\vec{r}_{A_1,P}|}{a} + \gamma q e\frac{|\vec{r}_{A_2}|}{a}\cos\Phi_P\right. \\
&+ (\gamma q - 1)(1-e^2) \\
&\left.+ (1-\gamma)(\mu+\frac{1}{2})(1-e^2)\frac{q}{1+q}\right],
\end{aligned} \tag{18}$$

$$\begin{aligned}
\left\langle\frac{de}{dt}\right\rangle_{\rm sec} = \;& \frac{(1-e^2)^{1/2}}{2\pi}\frac{\dot{M}_0}{M_1} \\
&\times\left[\gamma q\frac{|\vec{r}_{A_2}|}{a}\cos\Phi_P + \frac{|\vec{r}_{A_1,P}|}{a}\right. \\
&+ 2(\gamma q - 1)(1-e) \\
&\left.+ 2(1-\gamma)(\mu+\frac{1}{2})(1-e)\frac{q}{1+q}\right].
\end{aligned} \tag{19}$$

The rates of orbital evolution are thus linearly proportional to the magnitude $\dot{M}_0$ of the mass transfer rate at periastron and dependent on the orbital semi-major axis $a$, the orbital eccentricity $e$, the donor mass $M_1$, and the binary mass ratio $q$. They also depend on the donor's rotational angular velocity $\Omega_1$ through the position vector $\vec{r}_{A_1}$ of the inner Lagrangian point $L_1$ (e.g., Sepinsky et al. 2007a). Since $|\vec{r}_{A_1,P}| \propto a$, the timescales explicitly depend on the orbital semi-major axis $a$ only through the ratio $|\vec{r}_{A_2}|/a$ of the accretor's equatorial radius to the orbital semi-major axis. In the limiting case of conservative mass transfer ($\gamma = 1$), Eqs. (18) and (19) reduce to Eqs. (39) and (40) in Paper I.

In Figure 1, the evolutionary timescales $\tau_a = a/\dot{a}$ and $\tau_e = e/\dot{e}$ for the semi-major axis $a$ and orbital eccentricity $e$ due to mass transfer in an eccentric binary are shown as a function of the binary mass ratio $q$, for different values of the orbital eccentricity and the parameters $\gamma$ and $\mu$ [see Eqs. (2) and (3)]. While the actual timescales are given by the absolute values of $\tau_a$ and $\tau_e$, we here allow the timescales to be negative as well as positive to distinguish between negative and positive rates of change of the orbital elements.

For the calculation of the timescales, we assume the donor to rotate synchronously with the orbital angular velocity at periastron, and take the accretor to be a $1.44\,M_\odot$ neutron star. The donor mass is then fixed by the binary mass ratio. Since the radius of the neutron star is much smaller than the semi-major axis of the orbit, the terms in Eqs. (18) and (19) containing the ratio $|\vec{r}_{A_2}|/a$ are negligible compared to the other terms. We therefore set $|\vec{r}_{A_2}| = 0$, so that the timescales $\tau_a$ and $\tau_e$ are independent of $a$. For the mass transfer rate we adopt a constant $\dot{M}_0 = -10^{-9}\,M_\odot\,{\rm yr}^{-1}$, but note that the linear dependence of the rates of change of the orbital semi-major axis and eccentricity on $\dot{M}_0$ allows for an easy rescaling of the timescales to different mass transfer rates.

The overall shape of the curves shown in Figure 1 is similar to that of the curves shown in Figure 2 of Paper I in the case of conservative mass transfer. For a given fraction $\gamma$ of mass loss from the system, increasing $\mu$ implies more angular momentum loss from the binary, and thus faster orbital shrinkage or slower orbital expansion. For a given degree $\mu$ of specific orbital angular momentum loss, on the other hand, decreasing $\gamma$ implies more mass loss from the binary, causing faster orbital expansion and slower orbital contraction. The timescales for the evolution of the orbital eccentricity show a similar dependence on the parameters $\gamma$ and $\mu$.

The evolutionary timescales of the orbital semi-major axis $a$ and eccentricity $e$ can be negative as well as positive, depending on the initial binary properties. The transition from shrinking to growing orbital elements is illustrated more clearly by the contour plots shown in Figure 2. In these plots, the gray shades represent different timescales of orbital evolution and the thick black line marks the transition from shrinking (*right of the thick black line*) to growing (*left of the thick black line*) orbital elements. For comparison, the dashed black line marks the transition in the case of fully conservative mass transfer presented in Paper I[1]. As $\gamma$ decreases, more mass is lost from the system and the transition from negative to positive rates of change of the semi-major axis and eccentricity moves to larger mass ratios. Conversely, as $\mu$ increases, more angular momentum is lost from the sys-

[1] The sharp bend of the dashed line toward smaller $q$ values for $e \lesssim 0.95$ was not observed in Paper I due to the lower resolution of the orbital eccentricity grid considered in that paper. Equations (41) and (42) of Paper I still fit the line to better than 1.5% (10%) for $e \lesssim 0.8$ ($e \lesssim 0.95$) in the case of the orbital semi-major axis and for $e \lesssim 0.85$ ($e \lesssim 0.95$) in the case of the orbital eccentricity.

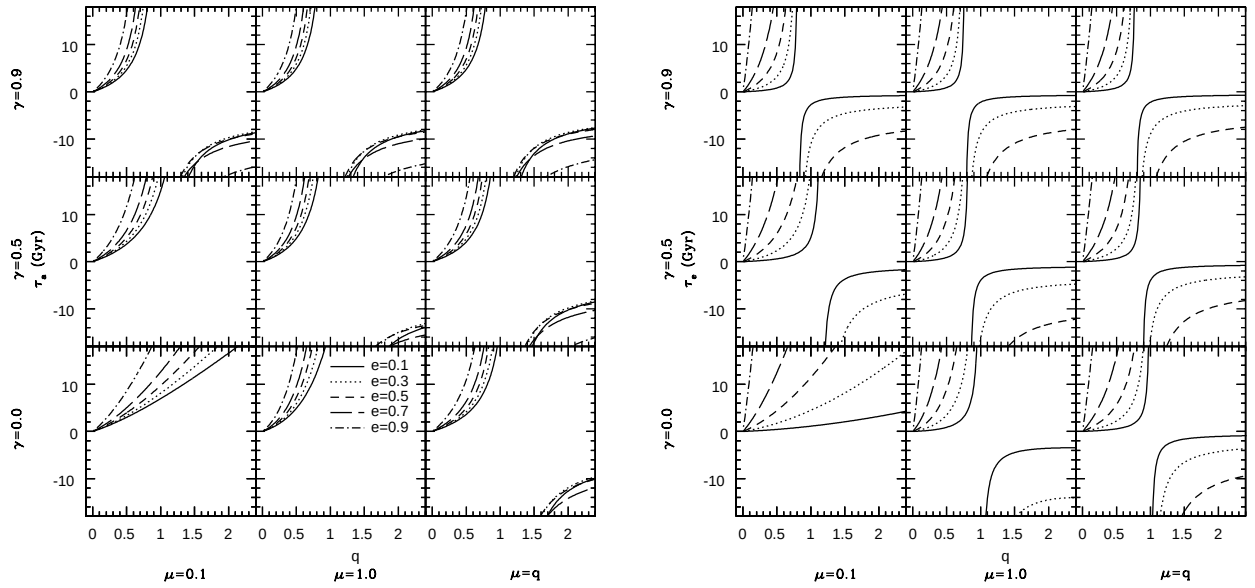


FIG. 1.— Orbital evolution timescales for the semi-major axis $a$ (*left*) and orbital eccentricity $e$ (*right*) for a delta function mass transfer rate $\dot{M}_1 = \dot{M}_0\,\delta(\nu)$ with $\dot{M}_0 = -10^{-9}\,M_\odot\,\mathrm{yr}^{-1}$. The timescales are calculated as a function of the binary mass ratio $q = M_1/M_2$ under the assumptions that the donor star rotates synchronously with the orbital angular velocity at periastron and that the accretor is a neutron star of mass $M_2 = 1.44\,M_\odot$. The different panels show timescales for different values of $\gamma$ and $\mu$. The $\mu = q$ panels correspond to the case where the matter lost from the system carries the specific orbital angular momentum of the accretor.

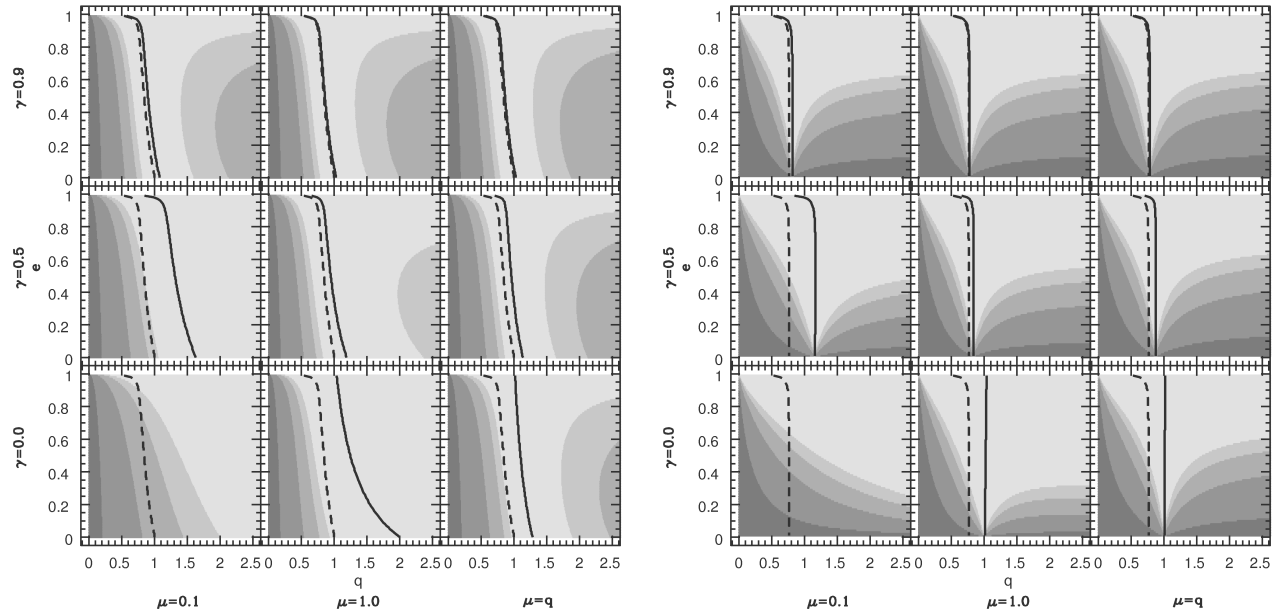


FIG. 2.— Contour plots of the orbital evolution timescales for the semi-major axis $a$ (*left*) and orbital eccentricity $e$ (*right*) in the $(q, e)$-plane for the same set of assumptions as adopted in Fig. 1. From the darkest to the lightest gray, the different gray shades represent timescales from 0 to 1 Gyr, 1 to 5 Gyr, 5 to 10 Gyr, 10 to 15 Gyr, and more than 15 Gyr, respectively. The thick black line in each panel separates the regions of the $(q, e)$ space where $\dot{a} > 0$ or $\dot{e} > 0$ (*left of the thick black line*) from the regions of the $(q, e)$ space where $\dot{a} < 0$ or $\dot{e} < 0$ (*right of the thick black line*). The timescales in the bottom left panel ($\gamma = 0$ and $\mu = 0.1$) are positive for all values of $q$ and $e$ displayed. For comparison, the dashed black line shows the dividing line between between increasing and decreasing orbital elements in the case of fully conservative mass transfer.

tem and the transition from negative to positive rates of change of the semi-major axis and eccentricity moves to smaller mass ratios. In the particular case where matter leaving the system carries away the specific orbital angular momentum of the accretor ($\mu = q$), the critical mass ratio separating increasing from decreasing orbital semi-major axes and eccentricities increases by about 30% when going from fully conservative to fully non-conservative mass transfer.

To assess the role of mass transfer in the overall evolution of the binary, we compare the timescales shown in Figures 1 and 2 with the orbital evolution timescales due to tidal dissipation in the Roche-lobe filling star. The tidal evolution timescales are determined as in Hurley et al. (2002) assuming the donor is a zero-age main-sequence star. The variations of the tidal evolution timescales as a function of the orbital eccentricity and binary mass ratio are shown in Figure 4 of Paper I. The discontinuity of the timescales at $q \simeq 0.87$ corresponds to the transition from donor stars in which convective damping is the dominant tidal dissipation mechanism ($M_2 \lesssim 1.25\,M_\odot$) to donor stars in which radiative damping is the dominant tidal dissipation mechanism ($M_2 \gtrsim 1.25\,M_\odot$).

The timescales of orbital evolution due to the combined effects of mass transfer and tides are shown as contour plots in Figure 3. As before, the thick black line indicates the transition from shrinking (*right of the thick black line*) to growing (*left of the thick black line*) orbital semi-major axis and eccentricity. For comparison, the transition line for conservative mass transfer is shown by means of the dashed black line. The vertical white line at $q \simeq 0.87$ separates donor stars in which tidal energy is dissipated by convective damping from donor stars in which tidal energy is dissipated by radiative damping. As noted in Paper I, in the case of conservative mass transfer, there are large regions in the $(q, e)$ parameter space where the combined effects of mass transfer and tidal interactions do *not* lead to rapid circularization of the orbit after the onset of mass transfer and where eccentricity pumping occurs instead of eccentricity damping. When mass loss from the system is taken into account, the parameter space for eccentricity pumping becomes even larger, though the timescales of orbital evolution in the newly accessible $\dot{e} > 0$ regions are long ($\gtrsim 15\,\mathrm{Gyr}$). Similar behavior is observed for the evolution of the orbital semi-major axis.

## 5. CONCLUDING REMARKS

We extended the formalism to study the orbital evolution due to mass transfer in eccentric binaries derived in Paper I to account for the effects of mass and angular momentum loss from the system. Adopting a delta function mass transfer rate at the periastron of the binary orbit, we find that the usually adopted assumption of rapid orbital circularization during the early stages of mass transfer remains unjustified when systemic mass and angular momentum loss are taken into account. Orbital eccentricities can therefore persist for observationally relevant periods of time.

The formalism presented in this paper and in Paper I can be incorporated into binary evolution and population synthesis code to provide a model for eccentric mass-transferring binaries which are currently, by construction, absent in any population synthesis studies of interacting binaries and their descendants. Possible applications include the modeling of systems such as Cir X-1 in which a neutron star is thought to accrete matter from a Roche-lobe filling or nearly Roche-lobe filling companion during each periastron passage and in which near-IR and X-ray spectroscopy support the presence of an accretion-driven mass outflow (Clark et al. 2003; Iaria et al. 2008; Tennant et al. 1986). Another example is the ultracompact X-ray binary 4U 1820-30 which is thought to be a member of a hierarchical triple (Chou & Grindlay 2001; Zdziarski et al. 2007). Futhermore, dynamical interactions between single and binary stars in dense stellar clusters can induce eccentricities in circular binaries and enhance eccentricities in already eccentric binaries (Heggie & Rasio 1996). This induced eccentricity can directly lead to Roche Lobe overflow at periastron, as has been suggested for the flaring X-ray binaries in NGC 4697 (Maccarone 2005). In future work, we intend to model the mass transfer rate at periastron more realistically by taking into account the atmospheric properties of the donor star and considering the feedback of the orbital and radial evolution of the star on the mass transfer rate.

This work is partially supported by NSF Award AST-0525995//ASW01 (subcontract from Adler Planetarium and Astronomy Museum), NSF CAREER Award AST-0449558, and NASA BEFS Award NNG06GH87G to VK. F.A.R. acknowledges support from NASA Grant NNG06GI62G. Numerical simulations presented in this paper were performed on the HPC cluster *fugu* available to the Theoretical Astrophysics Group at Northwestern University through NSF MRI grant PHY-0619274 to VK.

## REFERENCES

Brouwer, D., & Clemence, G. M. 1961, Methods of celestial mechanics (New York: Academic Press, 1961)
Chou, Y., & Grindlay, J. E. 2001, ApJ, 563, 934
Clark, J. S., Charles, P. A., Clarkson, W. I., & Coe, M. J. 2003, A&A, 400, 655
Danby, J. 1962, Fundamentals of celestial mechanics (New York: Macmillan, 1962)
Fitzpatrick, P. M. 1970, Principles of celestial mechanics (New York, Academic Press [1970])
Hadjidemetriou, J. D. 1969, Ap&SS, 3, 330
Heggie, D. C., & Rasio, F. A. 1996, MNRAS, 282, 1064
Hurley, J. R., Tout, C. A., & Pols, O. R. 2002, MNRAS, 329, 897
Iaria, R., D'Aí, A., Lavagetto, G., Di Salvo, T., Robba, N. R., & Burderi, L. 2008, ApJ, 673, 1033
Kolb, U., Rappaport, S., Schenker, K., & Howell, S. 2001, ApJ, 563, 958
Maccarone, T. J. 2005, MNRAS, 364, 971
Matese, J. J., & Whitmire, D. P. 1983, ApJ, 6, 776
Petrova, A. V., & Orlov, V. V. 1999, AJ, 117, 587
Raguzova, N. V., & Popov, S. B. 2005, ArXiv Astrophysics e-prints
Sepinsky, J. F., Willems, B., & Kalogera, V. 2007a, ApJ, 660, 1624
Sepinsky, J. F., Willems, B., Kalogera, V., & Rasio, F. A. 2007b, ApJ, 667, 1170

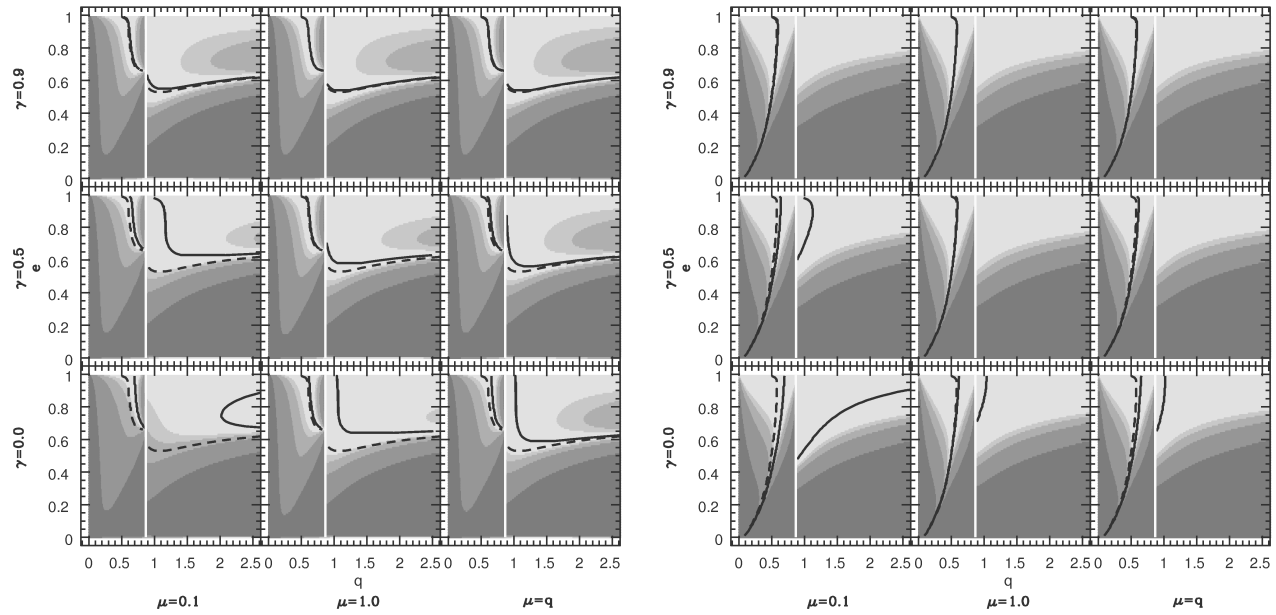


FIG. 3.— Contour plots of the orbital evolution timescales for the semi-major axis $a$ (*left*) and orbital eccentricity $e$ (*right*) in the $(q, e)$-plane due to the combined effects of mass transfer and tidal dissipation in the donor star of a semi-detached binary. The mass transfer rate is assumed to be a delta function of amplitude $\dot{M}_0 = -10^{-9}\, M_\odot\, \mathrm{yr}^{-1}$ at the periastron of the binary orbit, the donor star is assumed to rotate synchronously with the orbital angular velocity at periastron, and the accretor is assumed to be a $1.44\, M_\odot$ neutron star. The tidal contribution to the orbital evolution timescales is determined assuming the donor star has a radius equal to that of a zero-age main-sequence star of the considered mass. From the darkest to the lightest gray, the different gray shades represent timescales from 0 to 1 Gyr, 1 to 5 Gyr, 5 to 10 Gyr, 10 to 15 Gyr, and more than 15 Gyr, respectively. The thick black line in each panel separates the regions of the $(q, e)$ space where $\dot{a} > 0$ or $\dot{e} > 0$ (*left of the thick black line*) from the regions of the $(q, e)$ space where $\dot{a} < 0$ or $\dot{e} < 0$ (*right of the thick black line*). For comparison, the dashed black line shows the dividing line between between increasing and decreasing orbital elements in the case of fully conservative mass transfer. The vertical white line at $q \approx 0.87$ indicates the transition from convective damping (for $M_2 \lesssim 1.25\, M_\odot$) to radiative damping (for $M_2 \gtrsim 1.25\, M_\odot$) as the dominant energy dissipation mechanism.

Sterne, T. E. 1960, An introduction to celestial mechanics (Interscience Tracts on Physics and Astronomy, New York: Interscience Publication, 1960)

Tennant, A. F., Fabian, A. C., & Shafer, R. A. 1986, MNRAS, 221, 27P

Zdziarski, A. A., Wen, L., & Gierliński, M. 2007, MNRAS, 377, 1006

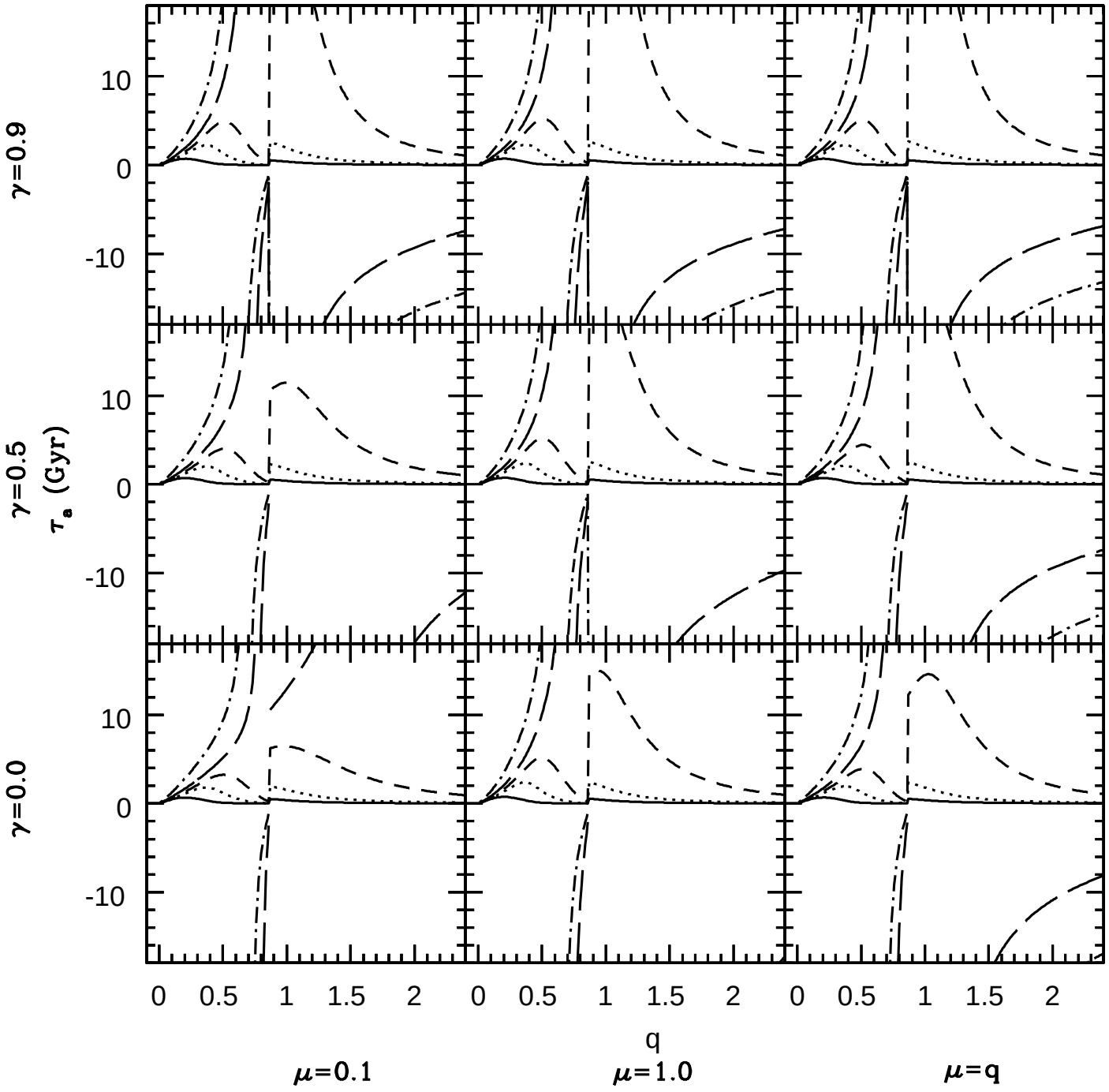
γ=0.9
γ=0.5
γ=0.0
τa (Gyr)
10
0
-10
0
0.5
1
1.5
2
q
μ=0.1
μ=1.0
μ=q

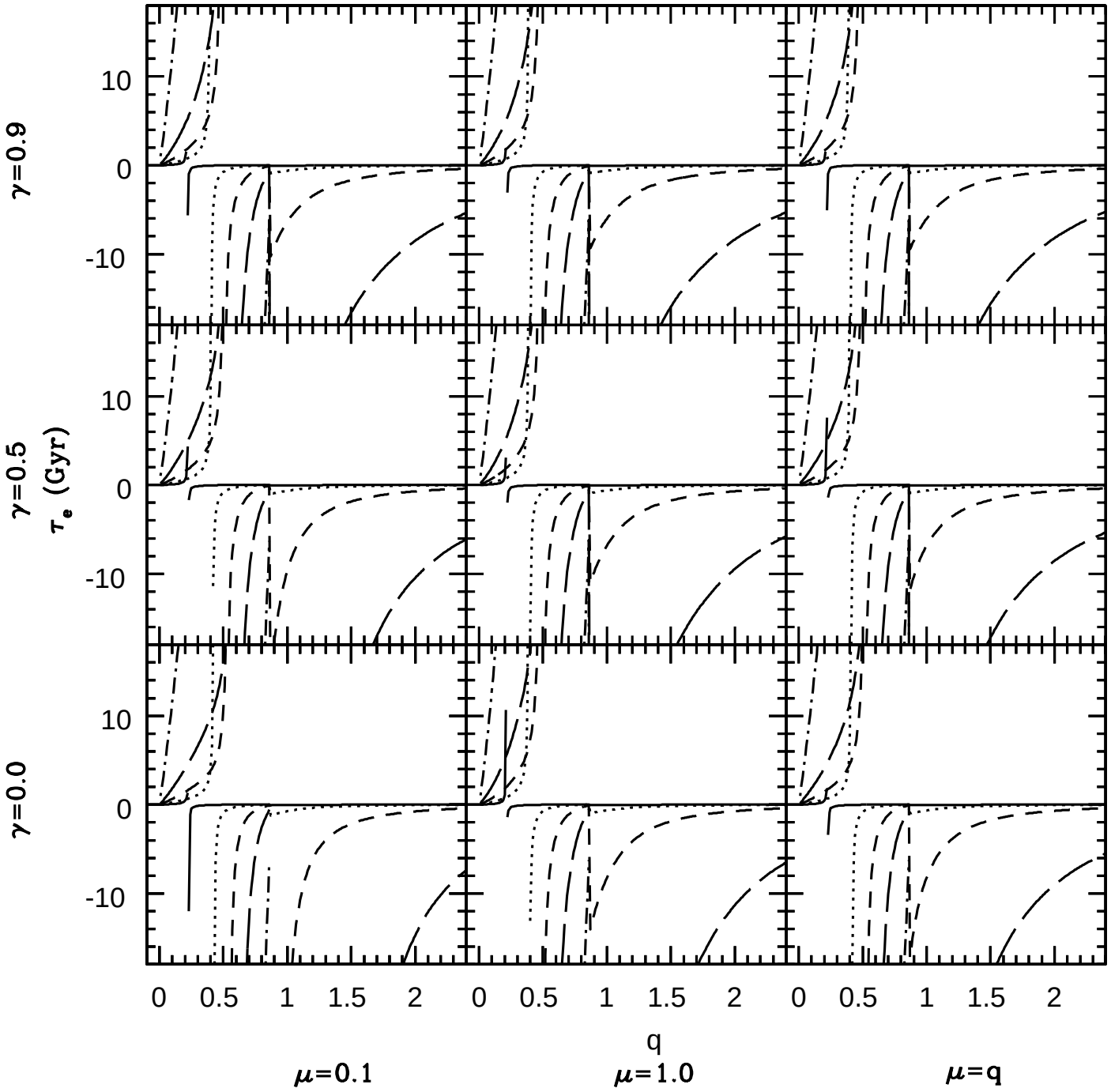
γ=0.9
γ=0.5
γ=0.0
τe (Gyr)
10
0
-10
0
0.5
1
1.5
2
q
μ=0.1
μ=1.0
μ=q